metadata, citation and similar papers at core.ac.uk

Accepted Manuscript

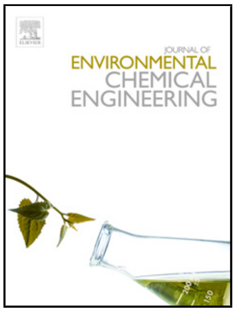

Title: Electrochemical bicarbonate reduction in the presence of Diisopropylamine on sliver oxide in alkaline sodium bicarbonate medium

Authors: Soraya Hosseini, Houyar Moghaddas, Salman Masoudi Soltani, Mohamed Kheireddine Aroua, Soorathep Kheawhom, Rozita Yusoff

PII: S2213-3437(18)30558-X
DOI: https://doi.org/10.1016/j.jece.2018.09.025
Reference: JECE 2646

To appear in:

Received date: 23-6-2018
Revised date: 10-9-2018
Accepted date: 16-9-2018

Please cite this article as: Hosseini S, Moghaddas H, Masoudi Soltani S, Kheireddine Aroua M, Kheawhom S, Yusoff R, Electrochemical bicarbonate reduction in the presence of Diisopropylamine on sliver oxide in alkaline sodium bicarbonate medium, *Journal of Environmental Chemical Engineering* (2018), https://doi.org/10.1016/j.jece.2018.09.025

This is a PDF file of an unedited manuscript that has been accepted for publication. As a service to our customers we are providing this early version of the manuscript. The manuscript will undergo copyediting, typesetting, and review of the resulting proof before it is published in its final form. Please note that during the production process errors may be discovered which could affect the content, and all legal disclaimers that apply to the journal pertain.

Electrochemical bicarbonate reduction in the presence of Diisopropylamine on sliver oxide in alkaline sodium bicarbonate medium

Soraya Hosseini[a,*], Houyar Moghaddas[b], Salman Masoudi Soltani[c],
,Mohamed Kheireddine Aroua[d], Soorathep Kheawhom[a], Rozita Yusoff[e]

[a]Computational Process Engineering Research Laboratory, Department of Chemical Engineering, Faculty of Engineering, Chulalongkorn University, Bangkok 10330, Thailand

[b]Department of Immunology and Physiology, Faculty of Arts and Science, University of Toronto, Ontario, Canada

[c]Department of chemical Engineering, College of Engineering, Design and Physical Sciences, Brunel University London, London UB8 3PH, United Kingdom

[d]Centre for Carbon Dioxide Capture and Utilization (CCDCU), School of Science and Technology, Sunway University, Bandar Sunway, 47500 Petaling Jaya, Malaysia

[e]Department of Chemical Engineering, University of Malaya, 50603 Kuala Lumpur, Malaysia

*Corresponding author‘s Tel: +60176515750
*Corresponding author‘s e-mail: Soraya.H@Chula.ac.ir

Abstract:

In this study, the reduction of bicarbonate in the presence four amines on a silver oxide/ carbon nanotube (Ag_2O/CNT) composite electrode has been investigated. The studied amines include ethanolamine (MEA), diethylenetriamine (DETA), diisopropylamine (DIPA) and aminoethylpiperazine (AEP). Regardless of amine type, in the absence of a bicarbonate solution, no reduction/oxidation peaks were observed. However, in the presence of bicarbonate, a single reduction peak along with simultaneous H_2 evolution was clearly observed. The cyclic voltammetry measurements showed that only diisopropylamine (DIPA) had a significant catalytic effect toward bicarbonate reduction on the composite electrode. No peak was observed in the anodic direction of the reverse scans, suggesting the irreversible nature of the electrochemical process. The effect of scan rate revealed that the irreversible reduction mechanism is governed by both diffusion and adsorption pathways. In addition of carbonate ions, format ions also have been detected in liquid phase. In order to study the mechanism of bicarbonate reduction in the DIPA solution on Ag_2O/CNT electrode, electrochemical impedance spectroscopy (EIS) was employed. The EIS results showed that the charge transfer resistance decreased when the potential decreased from -0.1 to -0.9 V then faded with a further rise in potential to up to -1.9 V. In addition, an inductive loop under certain conditions was observed in the complex plane due to the formation of adsorbed intermediates onto the electrode surface.

Keywords: Amines; Diisopropylamine; Silver oxide; Bicarbonate; Electrochemical Reduction;

Introduction:

Fossil fuel-fired power plants together with the incineration of waste materials are key contributors to carbon dioxide (CO_2) emissions. They make up of approximately 30% of total global CO_2 release into the atmosphere [1, 2]. The rapid rise in the atmospheric CO_2 concentration has led to devastating climate change and therefore, is a key environmental concern. The adverse effects of climate change such as ocean acidification, melting glaciers, rising sea levels (coastal erosion and flooding of low-lying land and cities), increasing severity of tropical storms and human health have been already felt worldwide [3-5]. Three strategies have been mainly explored: renewable energy sources and fuels that are less carbon-rich than the currently-favoured fossil fuels, limited but continued use of fossil fuels with the capture and storage of the associated CO_2 (CCS) and finally, conversion of CO_2 to other useful commodities such as cyclic-carbonates, methanol, ethanol and formic acid [6-8]. Aqueous solutions of amines interact with CO_2 and have been used for many years in the removal of CO_2 from gaseous streams. Amines are able to react with CO_2 molecules leading to reversible formation of carbamate, carbonate and bicarbonate species depending on the amine used. However, amine-based carbon capture processes demand high energy due to the amine regeneration and also inherits high capital and operating costs [9].

Among available carbon capture technologies, electrochemical reduction is a promising but less-studied method. This is mainly due to its benign operability under ambient reaction condition and easy controllability of the process via changing potential in order to produce different types of useful hydrocarbons [10, 11]. Recent studies on electrochemical transformation of CO_2 to other chemicals and renewable fuels have mostly employed electrolytes as the reaction media[12]. Several research works have been conducted to capture CO_2 in the presence of ionic liquids via electrochemical reduction[13,14]. Ionic liquids are shown to be appropriate electrolytes in various electrochemical devices. They exhibit negligible volatility, strong electrochemical stability and non-flammability [15,16]. Amine-impregnated adsorbents have been reported to enhance CO_2 capture alike. The amine-impregnated adsorbents exhibit improved photocatalytic performance in CO_2 photo-reduction which can be attributed to the enhanced CO_2 adsorption capacity. However, CO_2 and bicarbonate reduction have been rarely researched in the presence of amines and more specifically, through electrochemical reduction.

We have investigated the efficiency of four primary, secondary and tertiary amines in CO_2 (bicarbonate) capture through electrochemical reduction using an Ag_2O/CNT-coated nickel sheet composite electrode. Each amine demonstrated a distinct capability for bicarbonate reduction, owing to the variation in the number of amine groups and the asymmetric molecular structures of the studied amines. The effect of amine loading, scan rate, bicarbonate concentration and solution pH were all studied via cyclic voltammetry under ambient conditions. Electrochemical impedance spectroscopy (EIS) was used to study the interfacial processes on the surface of the composite electrode.

2. Experimental Procedures

2.1. Chemicals and Materials

Ethanolamine, diethylenetriamine, diisopropylamine and aminoethylpiperazine were purchased from Merck ltd. Sodium hydrogen carbonate (≥99.9999%), sulphuric acid and isopropanol (absolute ≥99.5%) were supplied by Everegreen Sdn Bhd. Ag_2O (99.99%), formic acid (98 wt%), KH_2PO_4 , $K_4Fe(CN)_6$ and Nafion solution (5 wt% dispersion in water) were bought from Sigma-Aldrich. Multi-walled carbon nanotubes (20−30 nm diameter, 0.5−2 μm length, >95% purity) were sourced from Nanostructured & Amorphous Materials ltd. Nickel sheet was purchased from a local supplier. All chemicals were used as received and without any further purification. Electrolyte solutions were prepared using ultrapure deionized water.

2.2. Electrochemical Reduction Process

Prior to the electrochemical reduction experiments, a composite electrode based on Ag_2O and carbon nanotube (CNT) was prepared by mixing Ag_2O (70 mg), CNT (30 mg), Nafion binder (5 μL) and isopropanol (5 ml). The mixture was then ultrasonically agitated for 30 minutes. A rectangular nickel sheet (1cm× 0.8cm) was used as the current collector. The Ni sheet was soaked in the ink solution. The composite electrode was then dried under ambient conditions (25 ^oC, 1atm). The entire surface of the nickel sheet was coated three times using the already-prepared Ag2O/CNT (70/30 wt%) ink. A full coated electrode was employed in the subsequent experiments. All experiments (cyclic voltammetry) were carried out in an electrochemical cell using three electrodes at room temperature and ambient pressure. An Autolab Metrohm Potentiostat electrochemical workstation, a Pt wire as the counter electrode and an Ag/AgCl (sat. KCl) as the reference electrode were used in the cyclic voltammetry (CV) experiments. A bicarbonate solution ($NaHCO_3$) represented the dissolved CO_2 due to the production of HCO_3^- ions upon dissolution in water (pH=7.3). In the next step, amine(10

%v/v amine/0.5M$NaHCO_3$) was introduced into the bicarbonate solution (pH=9.5). Cyclic voltammograms were measured at a scan rate of 0.05 V/s for a 0.5 M $NaHCO_3$ solution. Electrochemically-active surface area of the composite electrode Ag_2O/CNT (70/30 wt%) was estimated using chronoamperometry technique at the potential 0.3V. In order to measure the electrochemically-active surface area of the electrode, the chronoamprogram of a KH_2PO_4 solution (0.1 M) containing 5 mM K4Fe$(CN)_6$ as the redox probe was recorded. The electrochemical experiment on the composite electrode was performed using Autolab Metrohm potentiostat and NOVA 1.10 software. The electrochemical impedance spectroscopy (EIS) measurements were conducted using the frequency response module of the potentiostat (Alpha Analytical SP-300 with EC-Lab V10.12 software) under ambient pressure and temperature. The spectra were recorded at a cell potential of -2 to 1 V with an AC amplitude of 10 mV over a frequency range of 1 Hz to 200 kHz. The electrochemical reaction was carried out in the two compartments that the first one (working compartment with Ag_2O/CNT as working electrode and reference electrode), another compartment is with counter electrode. The concentration of the products were analysed via liquid chromatography using an HPLC (Shimadzu) at 25 °C fitted with a C18 column (4.6 mm 150 mm 5 μm) and coupled with a UV detector working at 210 nm. A mobile phase was prepared containing 8 mmol/L sodium sulphate and 1 mmol/L sulphuric acid. Prior to any sample injection (10 μL) into the HPLC, samples were filtered through a 0.25 mm membrane filter.

3. Results & Discussion

3.1 Cyclic Voltammetric Analysis

Carbon capture processes typically involve solvent-based (often amines) absorption of CO_2 followed by a solvent regeneration step in order to strip off the CO_2 and regenerate the solvent. Solvent regeneration process is costly and imposes significant energy penalties [9, 17]. Carbamate, carbonate, and bicarbonate species are produced during the absorption of CO_2 with amines. The ratios of these species depend on the type of amines (primary, secondary or tertiary) used. This study is to successfully integrate reduction reactions in order to convert these species into useful compounds such as hydrocarbons, green fuels and gaseous feeds for Fischer–Tropsch process. Four different types of amines i.e. ethanolamine(99%), diethylenetriamine(99%), diisopropylamine(99%) and aminoethylpiperazine(99%) were experimented in the presence of bicarbonate solution ($NaHCO_3$) as the CO_2 source. This simplifies the operation and allows for an accurate quantification of CO_2. The selected amines with their corresponding molecular structures are tabulated in Table 1; Aliphatic and heterocyclic amines with different structures were used in the present study. Ethanolamin is a primary while diethylenetriamine and diisopropylamine are secondary amines. On the other hand, aminoethylpiperazine comprise elements of primary, secondary and tertiary nitrogen atom.

Electrochemical reduction of bicarbonate solution was carried out using the composite Ag_2O/CNT (70/30 wt%) electrode. The cathodic reduction of the aliphatic and heterocyclic amines was studied under different conditions. Firstly, the chemical reductions of all the four amine solutions (CO_2-free) were separately examined which showed a very poor voltammetric response (Fig.1). No reduction or oxidation peaks were observed in the CV curves. Indeed, the amine molecules were not reduced at the cathode. Therefore, CO_2 (aq) (or a bicarbonate solution) is required to bind amines with CO_2. Several schemes have been proposed in the literature [18]:

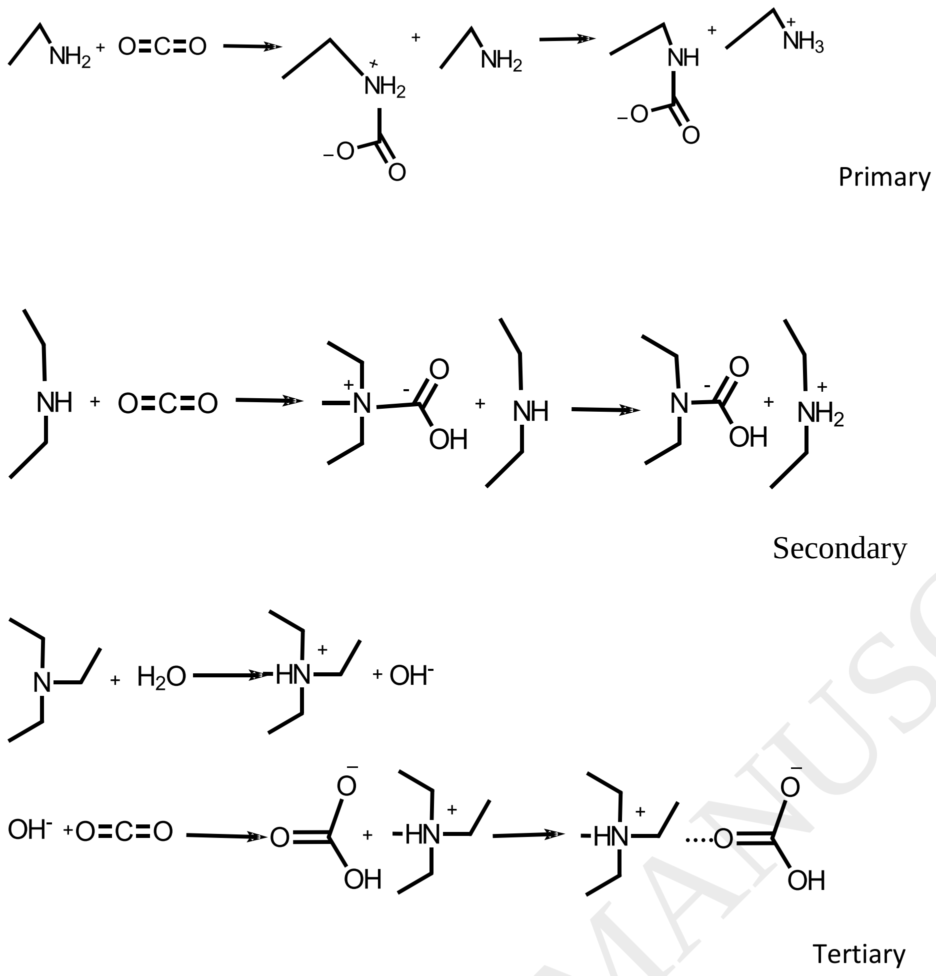

Scheme 1: The proposed suggestion for various amines with CO_2

In the presence of the bicarbonate solution (0.5 M $NaHCO_3$), a wide reduction peak was observed in the solution containing 10% v/v DIPA/0.5M $NaHCO_3$ while no considerable reduction was recorded for the bicarbonate solution mixed with the other amines (Fig.2)and (supplementary data Table S1). During the electrochemical reduction of $NaHCO_3$, the initial colourless solution was transformed into a coloured mixture. This was due to the formation of compounds when the three amines ethanolamine, diethylenetriamine and aminoethylpiperazine were employed in the electrochemical reduction by using the composite Ag_2O/CNT-coated Ni sheet electrode. A solution containing 10%v/v DIPA/$NaHCO_3$ was selected for further study.

The effects of amine loading (DIPA), bicarbonate concentration, solution pH and scan rate were investigated by using the composite electrode under ambient conditions. For these experiments, a known volume of amine solution (10 to 60 %v/v) was added to 0.5M $NaHCO_3$. It is seen (Fig 3) that the broad peak associated with the highest current density is generated when the amine loading sits at the minimum (10%v/v). A comparison of the onset potentials as a function of amine loading (using a composite electrode in 0.5M $NaHCO_3$) shows that the initial hydrogen evolution changes slightly with amine loading. In fact, an increase in amine volume leads to a decrease in the current density. This can be due to the diffusion-related limitation as the addition of more amine increases the solution viscosity, hindering diffusion and creating a hurdle for more bicarbonate to be reduced.

The effect of scan rate was studied for values from 0.01 to 0.2 V/s (Figure 4). It is seen that the reduction peaks are shifted to larger absolute potentials (i.e. from -0.38 to -1.1 V) with an increase in the scan rate from 0.01 to 0.2 V/s. When the scan rate increases, the peaks shift towards the negative direction with irreversible electrode reactions at higher scan rates. For the irreversible systems, the current density peak and the position of the potential are affected by reaction kinetics and its mechanism. The oxidation phase is almost uniform with a slight increase in its current intensity in lower scan rates, indicating a good stability of the reduced species. The peak-peak splitting is higher than 59 mV because the charge transfer rate is sluggish for a redox species. Scan rate studies were also conducted to decide whether the reaction process on the composite electrode is diffusion- or adsorption-controlled. In order to investigate whether the reduction process of 10%v/v DIPA/carbonate is predominantly diffusion- or adsorption-controlled, the regression coefficients associated with the linear plots of the reduction peak current versus the scan rate and the reduction peak current versus the square root of the scan rate were compared (figures are shown in supplementary data FS1). The latter revealed a linear relationship for scan rates between 0.01 and 0.2 V/s (Fig. 4) which is a typical feature of a diffusion-controlled process [19]. This equation is expressed as:

$$i_c = -59.08v^{0.5} - 29.917 \quad (r^2 = 0.892) \tag{1}$$

In addition, a logarithmic plot of the current (i_c) versus the scan rate (v) was produced and studied to determine the mechanism of the reduction reaction. A linear relation for scan rates from 0.01 to 0.2 V/s was obtained (Fig. 4) and expressed by the following equation:

$$\log(i_c) = 0.129\log(v) + 1.8 \quad (r^2 = 0.862) \tag{2}$$

The calculated line's slope above (i.e. 0.129) is not close to the theoretically-expected value of 0.5 for fully diffusion-controlled processes according to the Randles–Sevcik equation [19]. Therefore, it is concluded that the process is not fully diffusion-controlled at the Ag_2O/CNT surface for the applied potentials. The reduction reaction of 10%v/v DIPA/bicarbonate solution may follow the adsorption-related characteristics and that of the irreversible electrode process. Therefore, the intensity of the cathodic peak resulting from the reduction of the 10%v/v DIPA/bicarbonate should be proportional to the scan rate according to the Laviron equation [20] based on adsorption charge transfer. This linear relationship between i_c and v indicates that there is no diffusion limitation and that the reduction processes is mainly controlled by the charge transfer of the adsorbed species at the electrode surface. The relationship between the current and san rate gives the following linear equation:

$$i_c = -134.5v - 35.79 \quad (r^2 = 0.845) \tag{3}$$

The comparison between both plots shows that the current data is best fitted with the square root of the scan rate as confirmed by a better regression coefficient. Although the process is not completely diffusion-based, the diffusion mechanism demonstrates superiority to charge transfer mechanism. Therefore, there exists a combination of rate-limiting factors throughout this process: diffusion mechanism coupled with the partial adsorption of redox species onto the electrode surface. In addition to current, the potential of the reduction peak is also well dependent on the scan rate and shifts towards the larger absolute values with an increase in scan rate, suggesting the irreversibility of the reduction process [21]. A linear relationship between the peak potential and the logarithm of the scan rate (Fig. 4) is given by the following equation [22]:

$$E_{pc} = E_o - \frac{RT}{\alpha F}\left[0.78 + 2.303\ \log\left(\frac{(\alpha F\, D_o)^{0.5}}{K^o (RT)^{0.5}}\right)\right] - \frac{2.303\ RT}{\alpha F}\log v^{0.5} \tag{4}$$

$$E_{pc} = -2.9207 \log v^{0.5} - 0.0659 \quad (r^2 = 0.9831) \tag{5}$$

where E_o (V) is the formal potential of the reaction, α is the electron transfer coefficient, D_o is the diffusion coefficient (cm^2/s) and k_o is the standard heterogeneous rate constant (cm/s). By plotting E_{pc} versus log $v^{0.5}$ and calculating the slope of the line, a value of 0.22 was found for α. The two parameters k_o and E_o can be calculated from the intercept of equation (4) using a nonlinear regression. The values of k_o and E_o were found to be 6.04×10^{-4} cm/s and 0.123 V, respectively. The k_o value is resulted from concentration of redox active species and electron transfer to an electrode. The lager values of k_o indicate that the equilibrium between oxidation and reduction will be re-established quickly via an applied potential. The magnitude of standard heterogeneous rate constant depends on type and complexity of the molecules undergoing electron transfer, and also the molecular rearrangements due to electron transfer. The k_o values in accordance to reactions states are given as following[23]:

k_o 0.020 > k > 0.020 cm/s Reversible (6)

$k_o > 5.0 \times 10^{-5}$ k cm/s Quasi-reversible

$k_o < 5.0 \times 10^{-5}$ cm/s Irreversible

Formal potentials Eo is called conditional potentials to denote the reaction occurred under specified conditions rather than under standard conditions [24]. The obtained k_o value shows a quasi-reversible reaction for bicarbonate reduction in the presence DIPA.

The effect of bicarbonate concentration (0.1 to 1 M) is shown in Fig. 5. It can be seen that no reduction peak is measured with a bicarbonate concentration of 0.1 M. However, broad and sharp peaks were observed at concentrations of up to 1 M. Wide peaks are observed at concentrations from 0.3 to 0.5 M while sharp peaks are seen at concentrations from 0.7 to 1 M. With an increase in bicarbonate concentration, the peak potential shifts to the right and the baseline of the cathodic peak is well distorted. The peak current dependence on concentration indicates that the two peaks associated with the 0.3 M $NaHCO_3$ gradually merge into one single peak as the concentration increases. Such behaviour is a typical feature of the adsorption of the reactants. According to Randles–Sevcik equation, the current density is proportional to the surface concentration with an intercept of zero. However, the corresponding relationship between current density peak and surface concentration reveals a linear segment without crossing the origin as described with the following equation:

$$i_c = -22.3C - 18.01 \quad (r^2 = 0.917) \qquad (7)$$

This behaviour demonstrates a large deviation (i.e. the non-zero intercept), indicating the fact that in this process, the adsorption of species takes place on the surface of the electrode. Increasing the concentration of bicarbonate results in the saturation of electrode surface and the total charge flow during reduction reactions becomes constant. This is seen for bicarbonate concentrations from 0.7 to 1 M. Here, adsorption results in no noticeable change in the peak currents with an increase in concentration from 0.7 to 1 M which may be attributed to the complete coverage of the surface by the generated complex amine-bicarbonate that are absorbed on the catalyst surface. Amines with nitrogen atoms bound to either hydrogen or alkyl groups demonstrate significant basic properties due to the presence of the electron pair. By increasing $NaHCO_3$ concentration from 0.1 to 1 M, the initial pH of the 10%v/v DIPA/$NaHCO_3$ solution was decreased from 11.07 to 9.96, respectively. A slight drop in the pH value was observed after the reduction reaction and a decrease in basicity. This suggests the formation of acidic compounds in the solution. When sodium bicarbonate dissolved into water, the carbonic acid produced (exothermic process), however, carbonic acid is unstable due to release CO_2 and the process is significantly observed at high concentration bicarbonate. For this reason, no bubbling of CO_2 was observed in 0.5M $NaHCO_3$ and also the effects of the CO_2 bubbling caused a decrease in the pH of the electrolyte and affected the existence forms of the dissolved carbonaceous species. Therefor, 0.5M $NaHCO_3$ is considered for all experimental.

In order to enhance the efficiency of bicarbonate reduction, the effect of initial pH was studied in 10%v/v DIPA/0.5Mbicarbonate at a pH_i range of 8-11 and under an applied potential of -2 to 1 V. Figure 6 illustrates the influence of pH on bicarbonate reduction. No significant difference is seen among the measured reduction peaks. The influence of the pH can be expressed with respect to CO_3^{-2} or HCO_3^- species present in the solution as shown in Table 2. Zeebe and Wolf-Gladrow [25] showed that depending on the solution pH, different species were present in the Na_2CO_3/$NaHCO_3$ solutions with dissolved CO_2. These ions are mainly CO_2/CO_3^{2-}/HCO_3^- (pH=8), showing that most of the dissolved CO_2 is in the form of HCO_3^-. At pH=9, CO_2 converted to both HCO_3^- and CO_3^{2-} species and between pH 7 and 10, $HCO^-{}_3$ species dominates. By increasing pH to 10, CO_3^{2-} species dominate to HCO_3^- species and finally, almost complete dominance of CO_3^{2-} species at a pH of 11. Brito et al. investigated the effect of pH in reducing the CO_2 dissolved in alkaline solution of Na_2CO_3/$NaHCO_3$ [26]. They reported an optimum efficiency to be achieved at a pH of 8 due to adsorption of CO_2 and/or intermediates which consequently improves the transfer of electrons and protonation reaction. Figure 6 shows a small difference observed between the reduction peaks in pH values ranged from 8 to 11. This is an indication that the generated CO_3^{-2} species at higher pH values adversely affects the reduction process. The forward and reverse rate constants for the bicarbonate solution reactions are expressed as:

$$HCO_3^- \rightleftarrows H^+ + CO_3^{2-} \qquad k_f = 2.5\,\frac{1}{s}\ ,\ k_r = 5\times10^{-5}\,\frac{1}{Ms} \qquad (8)$$

$$HCO_3^- + OH^- \rightleftarrows H_2O + CO_3^{2-} \qquad k_f = 6\times10^{9}\,\frac{1}{Ms}, k_r = 1.2\,\frac{1}{s} \qquad (9)$$

It is seen that bicarbonate is dissociated into carbonate according to these two reactions.

In chronoamperometric studies, the current corresponding to the electrochemical reaction of ferrocyanide diffusing onto an electrode (0.3V) surface is described by Cottrell equation [27]:

$$I_= \frac{nFAD^{1/2}C_o}{(\pi t)^{1/2}} \qquad (10)$$

where I is current (A), *n* is number of electrons (1), A is the active area of the electrode (cm^2), F is the Faraday constant (96.487 C/mol), *D* and *Co* are the diffusion coefficient (6.20 ×10^{-6} cm^2/s) and the bulk concentration of $K_4Fe(CN)_6$ (5 X10^{-6} mol/cm^3), respectively[28]. Since the precise value of the diffusion coefficient of ferrocyanide is well known, the active surface area is estimated by plotting *I* vs $t^{-1/2}$ and the slope of the linear segment is used to calculate the surface area. The known information meet up with the standards for calculating surface area of electrode. The corresponding electro-active area was calculated to be 1.9464 cm^2. Since the geometric area is about 1.6 cm^2, an increase in surface area is an indication of a coarse and porous surface.

3.2 Impedance Analysis

In order to study the mechanism of bicarbonate reduction in the presence of DIPA on the Ag_2O/CNT electrode, electrochemical impedance spectroscopy (EIS) was employed (1 Hz – 200 kHz) for potentials ranging from -0.1 to -1.9 V. The high frequency intercepts on the x-axis of the Nyquist plot represent the electrolyte solution resistance. The diameter of the semi-circle represents the charge transfer resistance of the electrode (R_{ct}). The second semi-circle represents a resistance imposed by the reaction intermediates which are adsorbed/desorbed at the electrode surface. The Nyquist plot demonstrates a typical feature: semi-circles are observed at high frequencies which correspond to the electron transfer from liquid to solid. In addition, a linear section associated with the diffusion process is seen in the lower frequencies. Figure 7a illustrates the Nyquist plots for the 10%v/v DIPA/0.5M $NaHCO_3$ solution. The diameter of the semi-circle is slightly reduced by altering the potential from -0.1 to -0.9 V. As the value of the applied potential becomes more negative, the charge transfer resistance (R_{ct}) decreases from 2.89 to 1.85 Ω . This is evidenced by a decrease in the resistance value at intermediate frequencies. At low frequencies, the linear section begins to disappear by reducing the potential (no more diffusion reactants) and may be due to the accumulation of products preventing to diffuse the reactants into electrode surface. For the applied potentials, the Nyquist plot could be modelled by the well-known Randles electrical circuit [29]. The EIS data (Fig. 7a) suggests that the decreased electrical resistance (R_{ct}) may be caused by an increase in charge transfer and an increase in reduction efficiency. A typical model of the electrode–electrolyte interface in the presence of oxidation/reduction reactions are consist of three sections such as response of the interface, response due to electrochemical reactions and the response due to the electrolyte. Different chemical species at the electrolyte/electrode interfaces indicate the charge transfer is reduced from 2.85 to 1.89 Ω by reducing the potential, suggesting bicarbonate reduction caused the faster replies of faradaic processes that occur at the interface and the fast ion transfer behaviour (at reduction peak). Resistance (R_1) can be considered as a passive layer resistance attributed to accumulation of intermediate species. The minimum R1 value in the range -0.1 to -0.9V was observed around 7.34 Ω at -0.4V, indicating less accumulation of species at reduction potential. Electrolyte resistance is closely dependent on the number of charge carriers and their mobility within the electrolyte. It is seen that the charge resistance declines as the potentials moves from -0.1 to -0.9 V (with identical electrolyte resistance). The number of semi-circles and the presence of linear segments are dependent on the adsorption/absorption species, diffusion and hydrogen evolution. The Nyquist plot shows a small semi-circle at high-frequencies, a big semi-circle at middle frequencies and a linear section at low frequencies when a potential from -0.1 to -0.3 V is applied (onest peak). Here, the redox activity is initiated according to the CV. The appearance of the two semi-circles can be caused by the two different time constants. The first depressed semi-circles points out to the microscopic roughness on the surface of the solid electrode causing a heterogeneous distribution in the solution resistance. The semi-circle in the middle frequency region is related to the adsorption/absorption of reaction intermediate on the electrode surface together with H diffusion effects (part of a line) as seen in Fig. 7b. The Nyquist plot (Fig. 7c) shows the semi-circle in the middle frequency region at -0.4 V. Also, Warburg element has changed from semi-infinite diffusion to convective diffusion. When the reduction reaction is very fast, the semi-circle corresponding to adsorption disappears; however, the second semi-circle is observed for all other applied potentials. For potentials ranging from -0.5 to -0.9 V (endset peak), two semi-circles at high and middle frequencies, lacking a linear section, are observed. This corresponds to the adsorption/desorption limitations coupled with H_2 evolution (Fig 7d). In the applied potentials, the Bode plots contain two peaks (figures are shown supplementary FS2), indicating a two-step reduction mechanism: charge transfer and adsorption. The previously-mentioned effect of the scan rate also confirms this observation. The parameters were estimated using Z Fit software (EC lab 2) using the randomize/simplex fitting method to find the best fit between the model and the measured data. The most suitable set of parameter values is the one that yields the lowest χ^2 value and gives an estimation of the difference between the measured data and the fitted data (Table 3).

The semi-circle is associated with both the resistance and the capacitance. The constant-phase element was introduced instead of the double layer capacitance which illustrates the non-uniform distribution of capacitance over the electrode surface. Ions and water molecules adsorbed created double layer capacitance resulting from the potential difference between the electrodes suffering from electrolytic corrosion. Barbara et al. showed that capacitive EIS spectroscopy is an invaluable tool to obtain the surface coverage of species [30]. Capacitance plots have been used to obtain important information about electro-active thin films such as molecular surface coverage and electron transfer rates. The difference in capacitance observed for bicarbonate reduction can be used to characterize the nature of the species covering the surface. In the Nyquist plots, the capacitance (C) corresponds to the charge transfer increased when potential decreased from -0.1 to -0.8 V. The molecular coverage (Γ) can then be directly calculated from C by equation 11:

$$\Gamma = \frac{4RTC}{F^2 A} \tag{11}$$

The capacitance behaviour of the semi-circle shows that the molecular coverage has increased from 3.27×10^{-3} to 2.62×10^{-2} mol/cm^2 for applied potentials ranging from -0.1 to -0.4 V and then the molecular coverage drops to 2.25×10^{-6} mol/cm^2 for a potential of -0.9 V. The maximum surface coverage was estimated to occur at -0.48 V due to high fraction of the adsorption sites occupied on the electrode at the reduction peak. The decline in capacitance (i.e. -0.9 V) was observed due to pore blockage, hindering access of the electrolyte to the active sites. The rate constant for electron transfer (k_{et}) can be approximated from the frequency at the top of the semi-circle via the Cole–Cole or in the Bode capacitance plot as given in equation 12:

$$k_{et} = \Pi f_o \tag{12}$$

The rate constant for electron transfer (k_{et}) can be determined from the frequency f_0 (Hz) at the highest ordinate point in Bode capacitance plots (The plots were shown in

SupplementaryFS2). Equation 9 gives an electron transfer rate constant of k_{et} = 22.4 s^{-1} for the composite electrode at −0.4 V.

Figure 8a illustrates the Nyquist plots for 10 % v/v DIPA/0.5 M $NaHCO_3$ solution for applied potentials ranging from -1 to -1.9 V. It is seen that the semi-circles are not clearly observed and that the EIS responses at high frequencies display an inductive behaviour for the applied potential range (-1 to -1.9 V) with an H_2 evolution. The Nyquist plots measured at the potentials of -1 to -1.9 V comprise a capacitive loop in the high-frequency range and an inductive loop in the low-frequency range at the fourth quadrant. The existence of the inductive loop located in the fourth quadrant is due to the formation of adsorbed intermediates on the electrode surface. By decreasing the potential towards larger negative values, the Nyqusit plots appear to be considerably similar. Meyer et al. [31] stated that the inductive loops in EIS measurements carried out in an open-cathode stack are related to side reactions during the oxidation/reduction reaction phase. The electrical circuit was fitted to the EIS measurements through complex nonlinear regression methods for an applied potential of -1.1 V. A combination of parallel resistor, inductance and constant-phase element properly represents an electrode reaction process.

Stability (structure or cycling) as one of the most important parameters of electrode is considered. The stability of electrode was tested by Chronoamperometry (CA) measurements for 1000 s. The Ag_2O/CNT exhibited a decrease in the initial current in the 20s which was assigned to the adsorption of intermediate species that caused to block some active sites for bicarbonate reduction. The current decay on the electrode determines its efficacy in practical application. For cleaning of electrode after reduction reaction, a square wave voltammetry (SWV) in order to desorb poisoning species or intermediate species can be run (in supplementary dataFS3) and the current versus time increased significantly after SWV for cleaning.

3.3 Diisopropylamine reduction

A cathodic reduction peak appeared in the 10%v/v DIPA/0.5M $NaHCO_3$ solution at -0.48 V. The initial pH of the $NaHCO_3$ (0.5 M) solution was measured to be 7.3. The solution pH was increased to 9.5 by adding DIPA to bicarbonate solution(10%v/v). This confirmed that the HCO_3^- ions have reacted with the amine. Diisopropanolamine is a secondary amine which is bound to one proton and upon reaction with CO_2, produces carbamate and ammonium ions. The major constituents formed upon the dissolution of $NaHCO_3$ in water are OH^-, HCO_3^- and CO_3^{2-} ions. The concentration of bicarbonate ions increased and reached a maximum value at a pH of about 8.3. After this, the bicarbonate ions were converted to carbonate ions, a process which completed at a pH value of around 10.2. A solution containing 10%v/v DIPA/$NaHCO_3$ with a pH value of around 9.4 demonstrated the highest concentration of HCO_3^- ions in the solution and therefore, well reacted with the amine molecules. According to the literature [18], a mechanism has been proposed describing the absorption of CO_2 in secondary amine solutions and the formation a corresponding complex. Therefore, an increase in solution pH from 7.3 to 9.5 was observed by adding DIPA. After the completion of the reduction reaction, the solution pH slightly increased from 9.5 to 9.85, indicating that a fraction of bicarbonate in solution is, in fact, in carbonate form - particularly in lean amine solution. Carbamate, ammonium and HCO_3^- ions present in the solution are the constituents associated with the reduction reaction. In the absence of DIPA, the reduction reaction was carried out in the $NaHCO_3$ (0.5 M) solution by using Ag_2O/CNT. The solution pH was increased from 7.3 to 10.3, indicating that all bicarbonates were converted to carbonate ions. This owes to the fact that bicarbonate ions are, to a great extent, converted to carbonate at pH values greater than 8.3. After electrolysis at 60 mA for 3h, No significant amounts of formate products were detected through HPLC analysis in the liquid phase. The end point method via acid titration was employed for the solution of 10%v/v DIPA/0.5M$NaHCO_3$ before and after the reduction process. Three points at the pH values of 7.51, 5.11 and 3.02 were observed in 10%v/v DIPA/0.5M$NaHCO_3$ solution prior to the reduction reaction. After the reduction reaction, five points - 7.67, 6.51, 3.81, 2.15 and 2.09 - were recorded with two more points compared to the original solution.

Several methods were developed to determine the ions concentration on bicarbonate conversion. The estimation of the concentrations of carbonate and bicarbonate ions via the titration method (end point) was done before and after the reduction process according to equations below [32]:

$$[HCO_3^-]\left(\frac{meq}{L}\right) = \left(\frac{AlK - K_1 \times 10^{pH} + \frac{10^{-pH}}{\gamma}}{1 + 2K_2 \times 10^{pH}}\right) \tag{13}$$

$$[CO_3^{2-}]\left(\frac{meq}{L}\right) = \left(\frac{AlK - K_1 \times 10^{pH} + \frac{10^{-pH}}{\gamma}}{2 + \frac{10^{-pH}}{K_2}}\right) \tag{14}$$

$$[OH^-]\left(\frac{meq}{L}\right) = (K_1 \times 10^{pH}) \tag{15}$$

Where *Alk* is the computed sample alkalinity, *pH* is the initial pH of the sample, K_1 is the acid dissociation constant for water, K_2 is the second acid dissociation constant for H_2CO_3 and γ is the activity coefficient for H^+ (0.914). *Alk* is defined as the alkalinity of samples and is calculated by:

$$Alk = 1000 * V_t * N_a * C_F / V_o \tag{16}$$

Where Alk is the alkalinity of the sample (meq/L), V_t is the volume of titrant needed to reach the equivalence point (ml), N_a is the normality of the acid titrant, C_F is the acid correction factor and V_o is the initial volume of the sample (ml). The concentration of three constituents can be determined for the two cases; before and after the reduction reactions. The alkalinity values were found to be 630.11 and 770.31 meq/L for 10%v/v DIPA/0.5M$NaHCO_3$ before and after reduction process, respectively. The results of the titration analysis showed that $NaHCO_3$ (0.5 M) comprised OH^-, HCO_3^- and CO_3^{2-} ions with the values of 2.511×10^{-2} , 509964 and 120155 meq/L, respectively. After the reduction reaction, the values of 6.30×10^{-2}, 483915 and 286399 meq/L were recorded for OH^-, HCO_3^- and CO_3^{2-} ions, respectively. The pKa value was calculated from the Henderson-Hasselbalch equation as:

$$pK_a = pH + Log\left(\frac{HA}{A^-}\right) \tag{17}$$

For converting bicarbonate to carbonate ions, a pK_a value of 10.35 was reported and according to equation14, a pK_a value of 10.02 was found for the reduction products. The pH value 9.85 is smaller than the pKa (i.e. 10.02), indicating that it is mainly a protonated acid. The reduction efficiency (RE%) is a measurement on how much of the bicarbonate have been reduced to carbonate. At optimum condition, a reduction efficiency around 56% was resulted, suggesting inactivity catalyst due to adsorption of intermediate species may be considered as an important factor.

Conclusion

A composite Ag_2O/CNT-based electrode was employed to reduce carbonate to useful end products in the presence of four different classes of aqueous amines. The reduction process was seen to be irreversible since no oxidation peak was observed. The peaks shifted toward larger absolute values with increasing the scan rate re-confirming the irreversible nature of the reduction process. Among the studied amines, only diisopropylamine (DIPA) has showed a good reduction capability in the presence of bicarbonate solution with a peak centered at potential -0.5V. The effect of the scan rate suggests that both the diffusion and adsorption mechanisms are playing important roles in the reduction of carbonate ions in the presence of diisopropylamine (DIPA). In addition to carbonate formation, no significant amount of format was detected in the liquid phase. The EIS results were analysed using Nyquist and Bode plots and were used to determine both the molecular coverage (Γ) and the heterogeneous electron transfer rate constant (k_{et}) with the values of 2.62×10^{-2} mol/cm^2 and 22.4 s^{-1} for the composite electrode at reduction potential, respectively.

Acknowledgment

This research is supported by Rachadapisek Sompote Fund for postdoctoral Fellowship, Chulalongkorn University.

References:

[1] Gopalram Keerthiga, Balasubramanian Viswanathan, Raghuram Chetty, Electrochemical reduction of CO_2 on electrodeposited Cu electrodes crystalline phase sensitivity on selectivity, Catal. Today 245 (2015) 68–73.

[2] Niall MacDowell, Nick Florin, Antoine Buchard, Jason Hallett, Amparo Galindo, George Jackson, Claire S. Adjiman, Charlotte K. Williams, Nilay Shahb,Paul Fennell, An overview of CO2 capture technologies, Energy Environ. Sci. 3(2010)1645–1669.

[3] Lixin Zhang , Na Li , Hongfang Jiu , Guisheng Qi , Yunjie Huang, ZnO-reduced graphene oxide nanocomposites as efficient photocatalysts for photocatalytic reduction of CO_2, Ceram. Int., 41 (2015)6256–6262.

[4]Byoungsu Kim, Sichao Ma, Huei-Ru Molly Jhong, Paul J.A. Kenis, Influence of dilute feed and pH on electrochemical reduction of CO2 to CO on Ag in a continuous flow electrolyzer, Electrochim. Acta ,166 (2015) 271–276.

[5] F. Niazmehr, H. Fathi, A.R. Ansari, A.R. Dijirsarai, A.R. Pendashteh, Reduction of chloride ions in the diethanol amine cycle and improvement of the natural gas sweetening, J. Nat. Gas Sci. Eng., 31 (2016) 730-737.

[6] Michael R. Thorson, Karl I. Siil, Paul J. A. Kenis, Effect of cations on the electrochemical conversion of CO_2 to CO, J. Electrochem. Soc., 160(2013) F69-F74.

[7] Claire E. Tornow, Michael R. Thorson, Sichao Ma, Andrew A. Gewirth, Paul J. A. Kenis, Nitrogen-based catalysts for the electrochemical reduction of CO_2 to CO, J. Am. Chem. Soc. 134 (2012) 19520-19523.

[8] Eric J. Dufek, Tedd E. Lister,Michael E. McIlwain, Influence of electrolytes and membranes on cell operation for syn-gas production, Electrochem. Solid State Lett. 15 (2012) B48-B50.

[9]Cheng-Hsiu Yu, Chih-Hung Huang, Chung-Sung Tan,A Review of CO2 Capture by Absorption and Adsorption, Aerosol and Air Quality Research, 12 (2012)745–769.

[10]Ruud Kortlever, Jing Shen, Klaas Jan P. Schouten, Federico Calle-Vallejo, Marc T. M. Koper,Catalysts and Reaction Pathways for the Electrochemical Reduction of Carbon Dioxide, J. Phys. Chem. Lett., 6 (2015)4073–4082.

[11]D. DeCiccio, S.T. Ahn, S. Sen, F. Schunk, G.T.R. Palmore, C. Rose-Petruck, Electrochemical reduction of CO_2 with clathrate hydrate electrolytes and copper foam electrodes, Electrochem. Commun. 52 (2015)13–16.

[12] Abdalaziz Aljabour , Halime Coskun , Dogukan Hazar Apaydin , Faruk Ozel , Achim Walter Hassel , Philipp Stadler , Niyazi Serdar Sariciftci , Mahmut Kus, Nanofibrous cobalt oxide for electrocatalysis of CO_2 reduction to carbon monoxide and formate in an acetonitrile-water electrolyte solution, Appl. Catal. B: Environ.l 229 (2018) 163–170.

[13] Maxime Mercy, Nora H. de Leeuw, Robert G. Bell, Mechanisms of CO2 capture in ionic liquids: a computational perspective, Faraday Discuss.,192(2016)479-492.

[14] X.P. Zhang, X. C. Zhang, Haifeng Dong, Zhijun Zhao, S. J. Zhang, Ying Huang, Carbon Capture with Ionic Liquids: Overview and Progress, Energy Environ. Sci. 5(2012)6668-6681.

[15] M. Alvarez-Guerra, J. A. Enrique Alvarez-Guerraa, A. Irabiena, Ionic liquids in the electrochemical valorisation of CO_2 , Energy Environ. Sci., 8(2015)2574-2599.

[16]Yeonji Oh, Xile Hu, Ionic liquids enhance the electrochemical CO2 reduction catalyzed by MoO_2, Chem. Commun, 51(2015)13698-13701.

[17] Patricia Luis , Use of monoethanolamine (MEA) for CO2 capture in a global scenario: Consequences and alternatives, Desalination 380(2016)93–99.

[18] Sunho Choi, Jeffrey H. Drese, Christopher W. Jones, Adsorbent materials for carbon dioxide capture from large anthropogenic point sources , ChemSusChem 2 (2009) 796–854.

[19]Soraya Hosseini, Soorathep Kheawhom, Salman Masoudi Soltani, Mohamed Kheireddine Aroua, Electrochemical reduction of bicarbonate on carbon nanotube-supported silver oxide: An electrochemical impedance spectroscopy study, Journal of Environmental Chemical Engineering 6 (2018) 1033–1043

[20]Lida Fotouhi , Maryam Fatollahzadeh, Majid M. Heravi, Electrochemical Behavior and Voltammetric Determination of Sulfaguanidine at a Glassy Carbon Electrode Modified With a Multi-Walled Carbon Nanotube, Int. J. Electrochem. Sci., 7(2012)3919 – 3928.

[21]Aamir Hassan Shaha, Waqar Zaida, Afzal Shaha,b,z, Usman Ali Ranac, Hidayat Hussaind, Muhammad Naeem Ashiqe, Rumana Qureshia, Amin Badshaha, Muhammad Abid Ziaf and Heinz-Bernhard Kraatzb, pH Dependent Electrochemical Characterization, Computational Studies and Evaluation of Thermodynamic, Kinetic and Analytical Parameters of Two Phenazines, J. Electrochem Soc, 162 (2015) H115-H123.

[22]Allen J. Bard, Larry R. Faulkner, Electrochemical methods Fundamentals and Applications , JOHN WILEY & SONS, INC. New Yorke, SECOND EDITION

[23] Helmut Kaesche, Corrosion of Metals: Physicochemical Principles and Current Problems, Springer, Berlin, Heidelberg (2003)75-118

[24]Scholz, F. In Electroanalytical Methods: Guide to Experiments and Applications; Scholz, F., Ed.; 2nd ed.; Springer: Berlin; 210(2010),Second Edition

[25] R. E. Zeebe, D. Wolf-Gladrow, CO2 in seawater: equilibrium, kinetics and isotopes, Amsterdam: Elsevier Science, 65(2001)360

[26] J. Ferreira de Brito, A.A. Silva, A.J. Cavalheiro, M. V. Boldrin Zanoni, Evaluation of the Parameters Affecting the Photoelectrocatalytic Reduction of CO_2 to CH_3OH at Cu/Cu2O Electrode, Int. J. Electrochem. Sci., 9 (2014) 5961 – 5973.

[27] Jan CMyland , Keith BOldham, Cottrell's equation revisited: an intuitive, but unreliable, novel approach to the tracking of electrochemical diffusion, Electrochem. Commun. 6(2004)344-350

[28] M.A. Ajeel, M.K. Aroua, W.M. A. Wan Daud , P-Benzoquinone Anodic Degradation by Carbon Black Diamond Composite Electrodes, Electrochim. Acta 169 (2015) 46–51.

[29] D. Yang, Q. Li, F. Shen, Q. Wang, L. Li, N. Song, Y. Dai, J. Shi, Electrochemical Impedance Studies of CO2 Reduction in Ionic Liquid/ Organic Solvent Electrolyte on Au Electrode, Electrochim. Acta, 189 (2016) 32–37

[30] B.P. G. Silva, D.Z. de Florio, S. Brochsztain, Characterization of a Perylenediimide Self-Assembled Monolayer on Indium Tin Oxide Electrodes Using Electrochemical Impedance Spectroscopy, J. Phys. Chem. C 118(2014)4103−4112.

[31] Jeremy P. Meyers, Marc Doyle, Robert M. Darling ,John Newman, The Impedance Response of a Porous Electrode Composed of Intercalation Particles, J. Electrochem. Soc. 147(2000) 2930-2940

[32] Frank M. Dunnivant, Environmental Laboratory Exercises for Instrumental Analysis and Environmental Chemistry, 28 JAN 2005, John Wiley & Sons, Inc

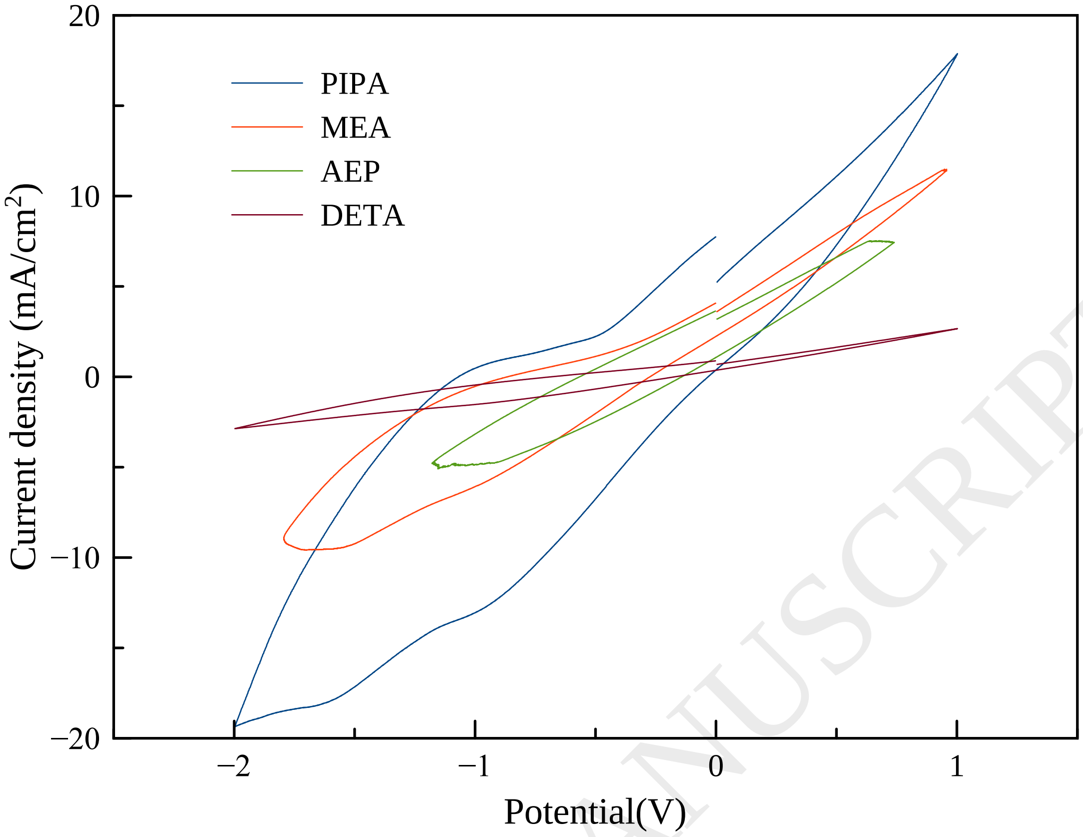

Figure 1 Cyclic voltammograms for various pure amines(99%) without carbonate solution in the range 1 to -2 V vs. Ag/AgCl

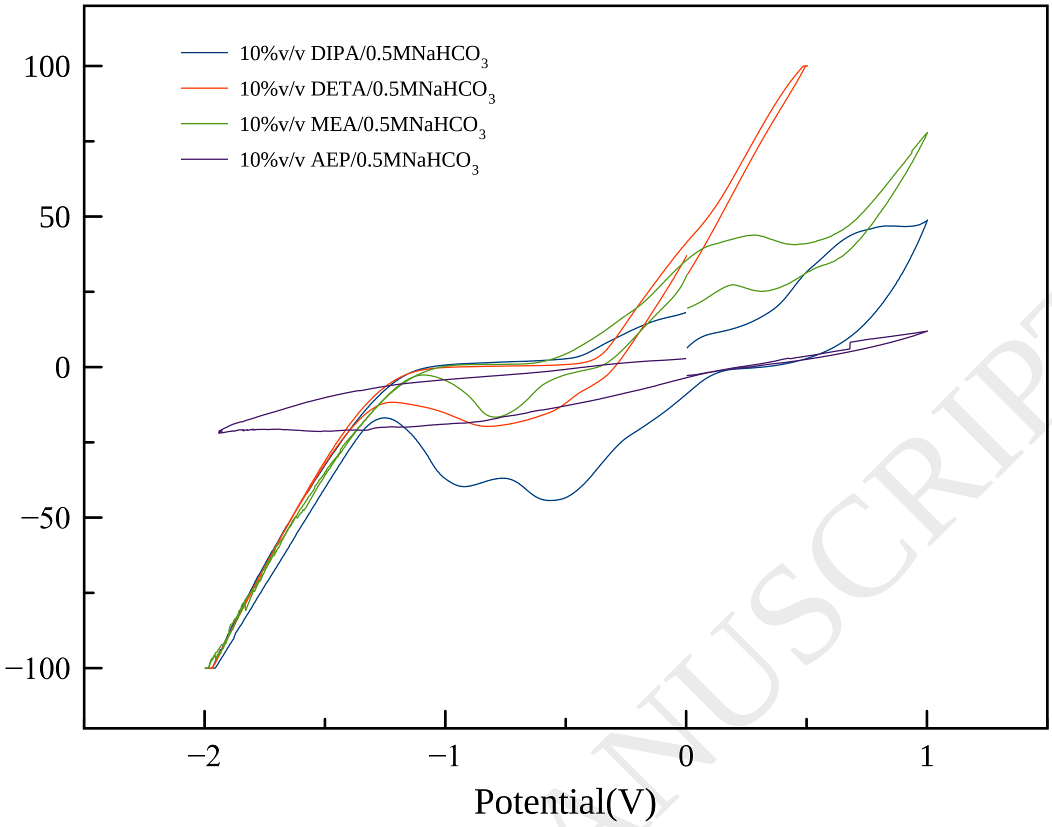

Figure 2 Cyclic voltammograms for various amines in the presence bicarbonate solution $NaHCO_3$ (10% v/v amine/$NaHCO_3$) in the range 1 to -2 V vs. Ag/AgCl

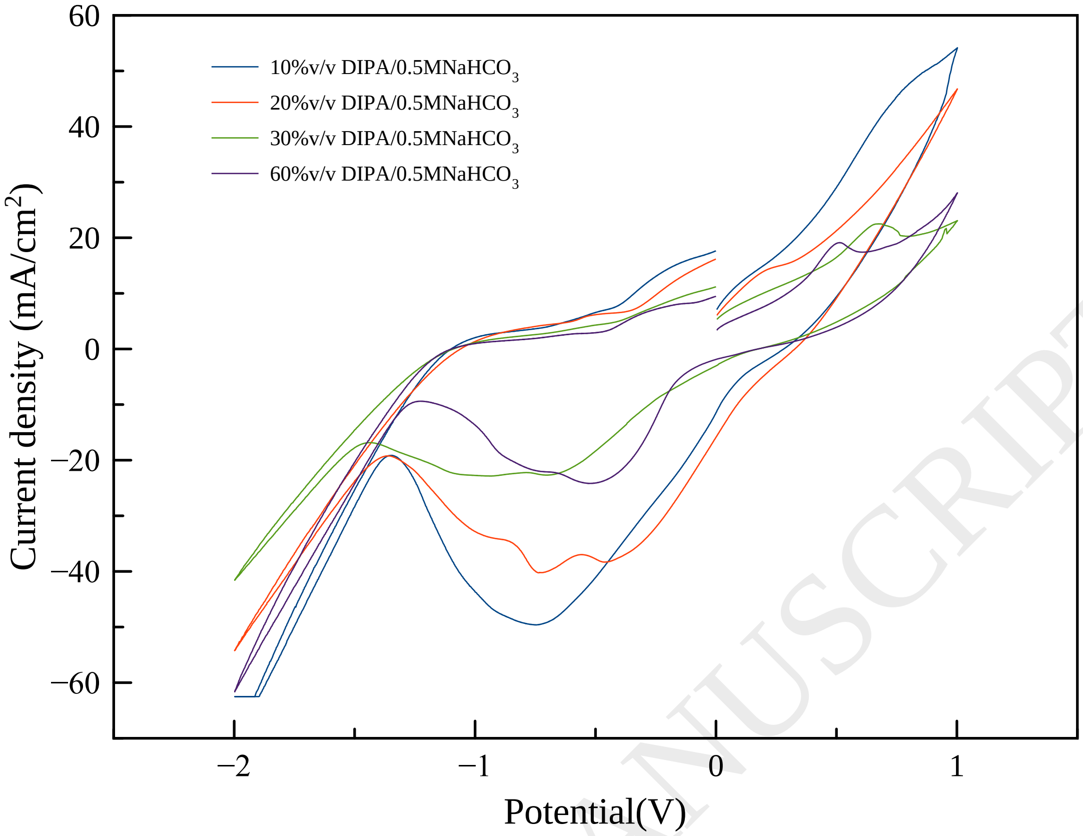

Figure 3 The effect of amine loading (DIPA) in the presence 0.5NaHCO$_3$ in the range 1 to -2 V vs. Ag/AgCl

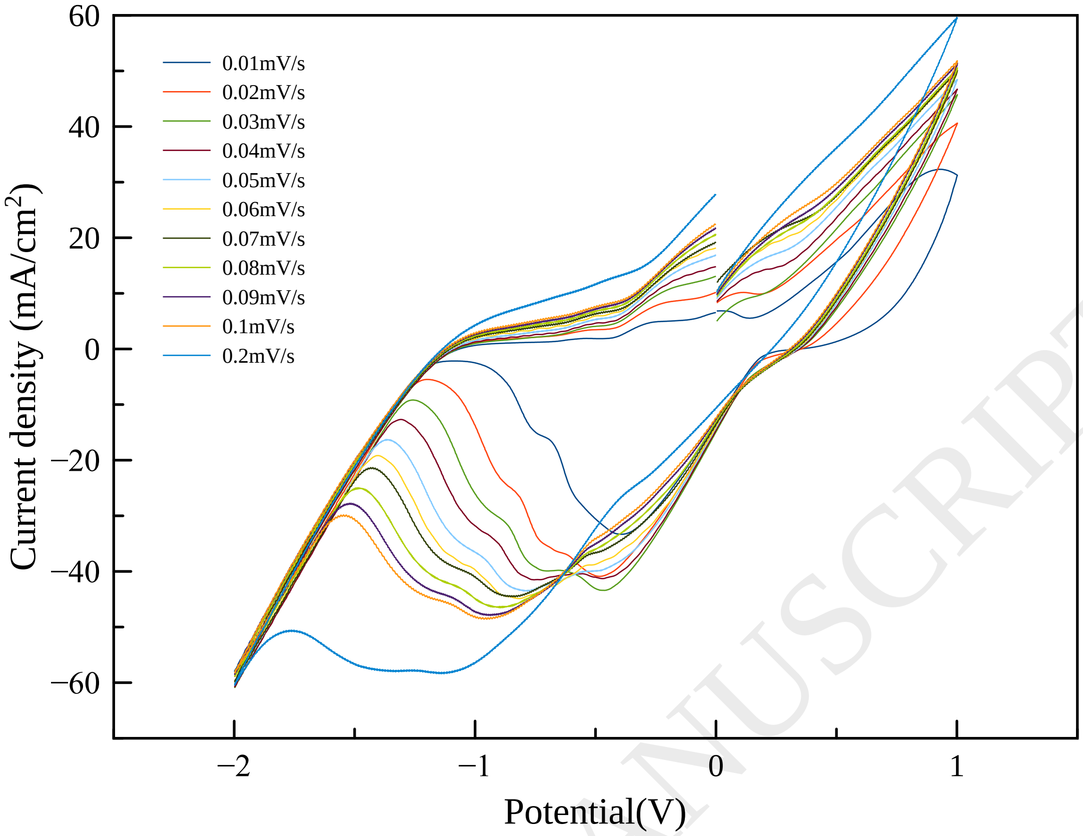

Figure 4 The effect of scan rate in 10%v/v DIPA/0.5NaHCO$_3$ in the range 0.01 to 0.2 V/s

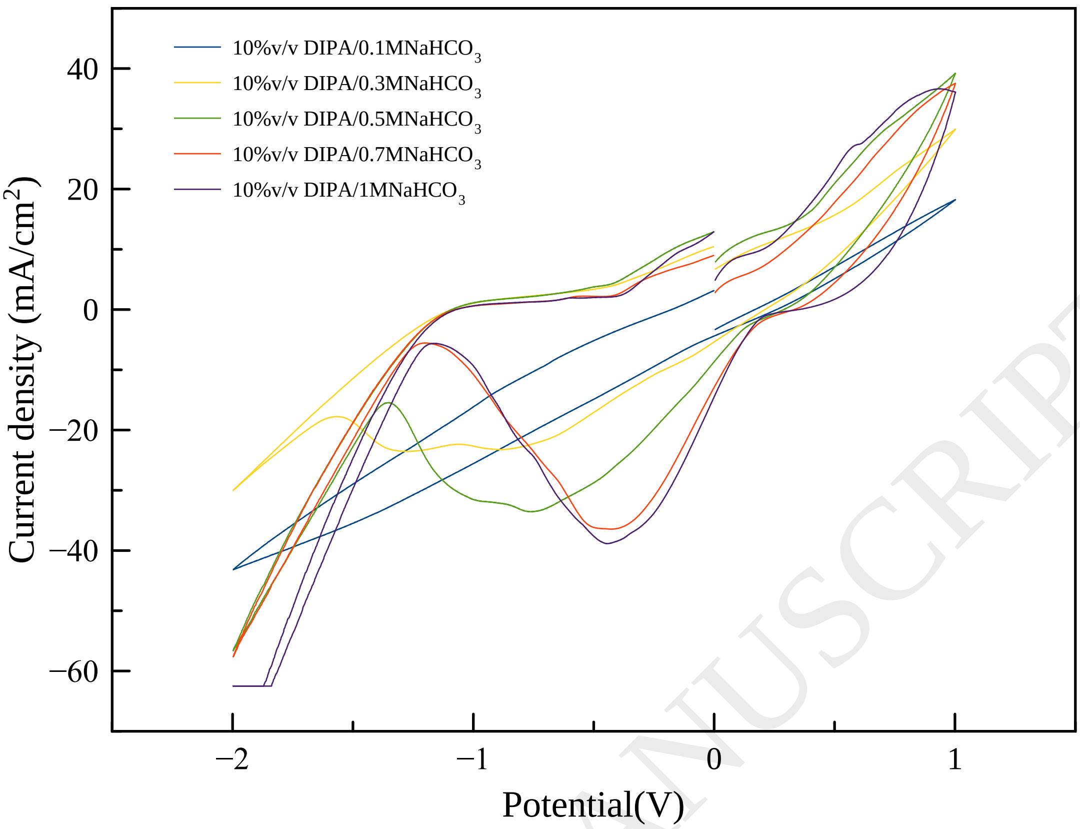

Figure 5 The effect of carbonate concentration in DIPA/NaHCO$_3$ in the range 0.1 to 1M

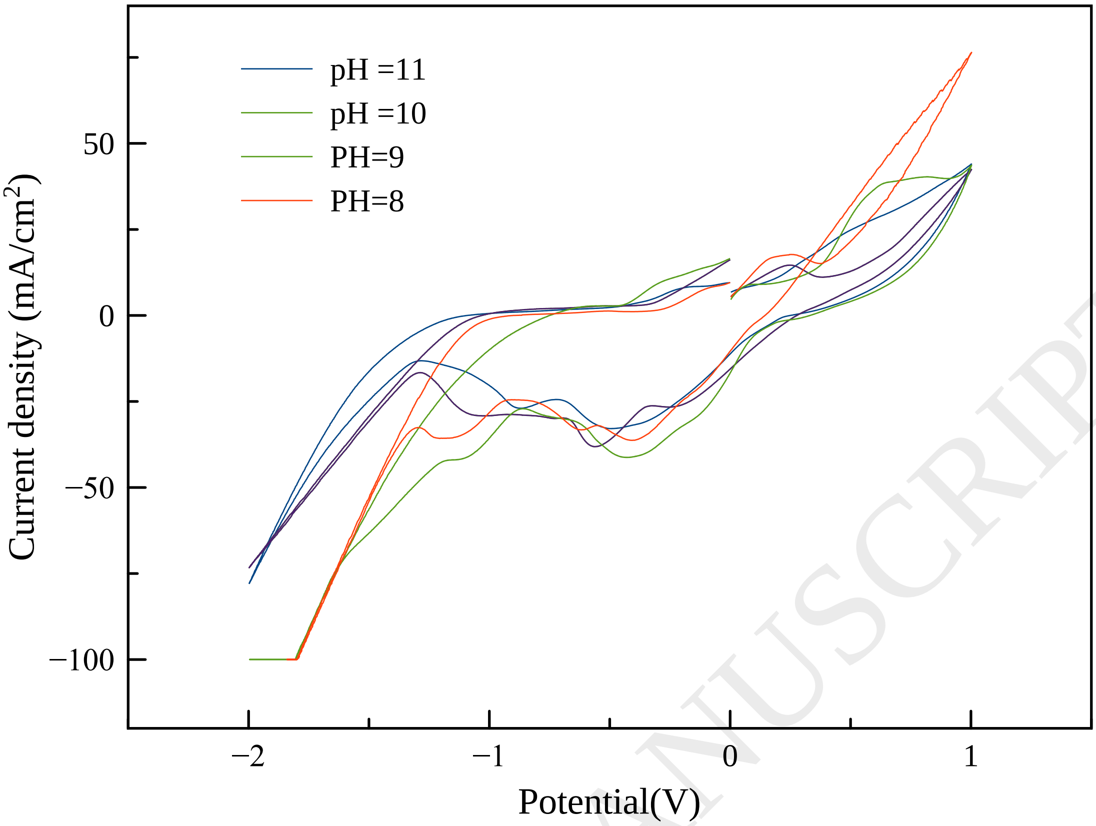

Figure 6 The effect of pH solution in DIPA/0.5 MNaHCO$_3$ in the range 8 to 11.

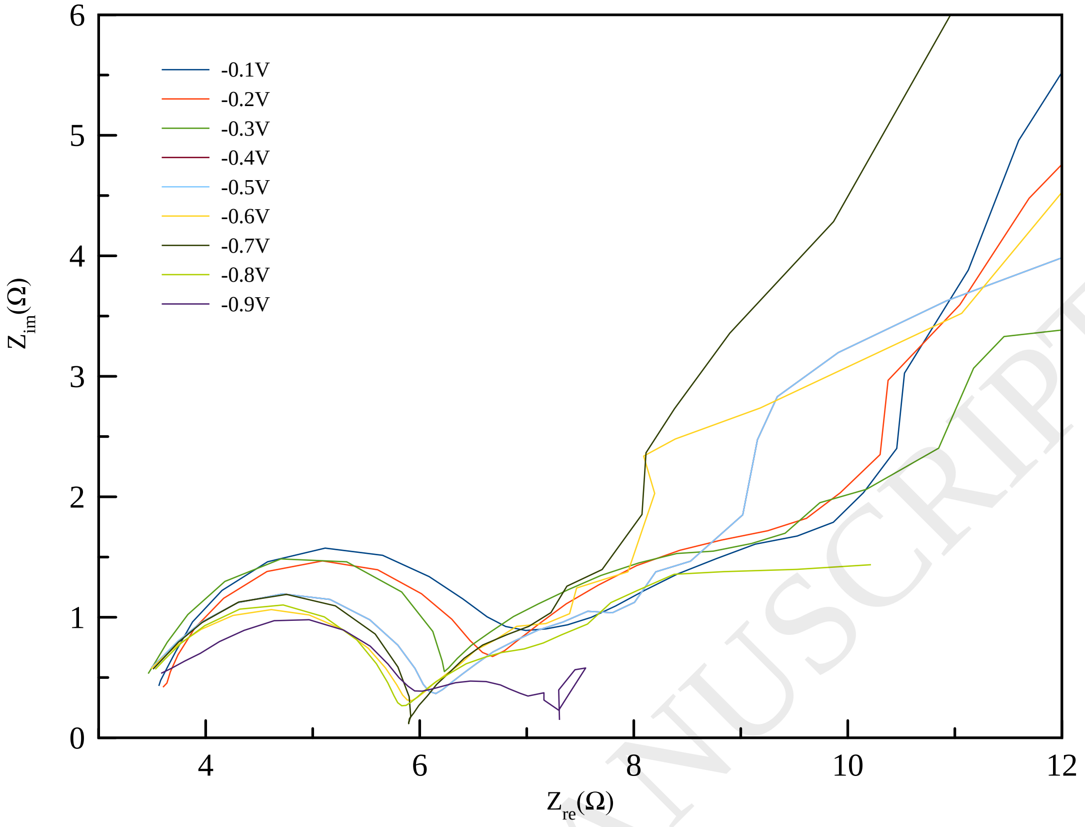
-0.1V
-0.2V
-0.3V
-0.4V
-0.5V
-0.6V
-0.7V
-0.8V
-0.9V
0
1
2
3
4
5
6
4
6
8
10
12
$Z_{im}(\Omega)$
$Z_{re}(\Omega)$

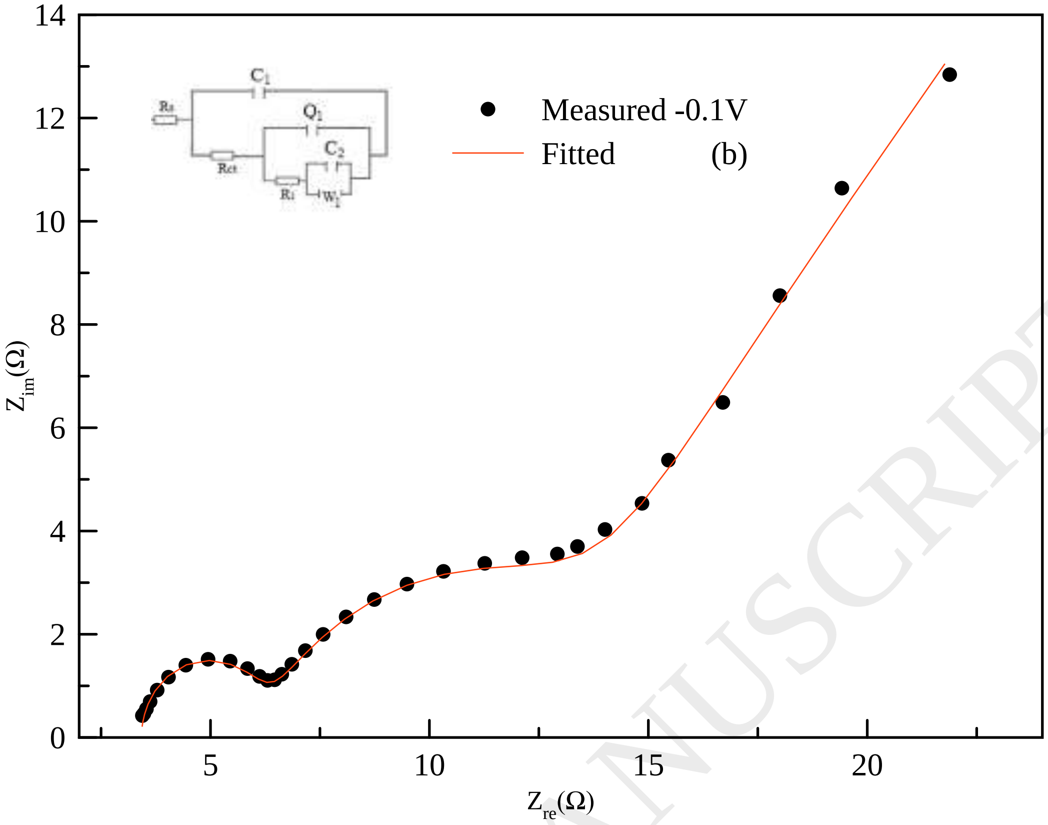
14
12
10
8
6
4
2
0
5
10
15
20
$Z_{im}(\Omega)$
$Z_{re}(\Omega)$
● Measured -0.1V
Fitted
(b)
Rs
C_1
Q_1
Rct
C_2
Ri
W_1

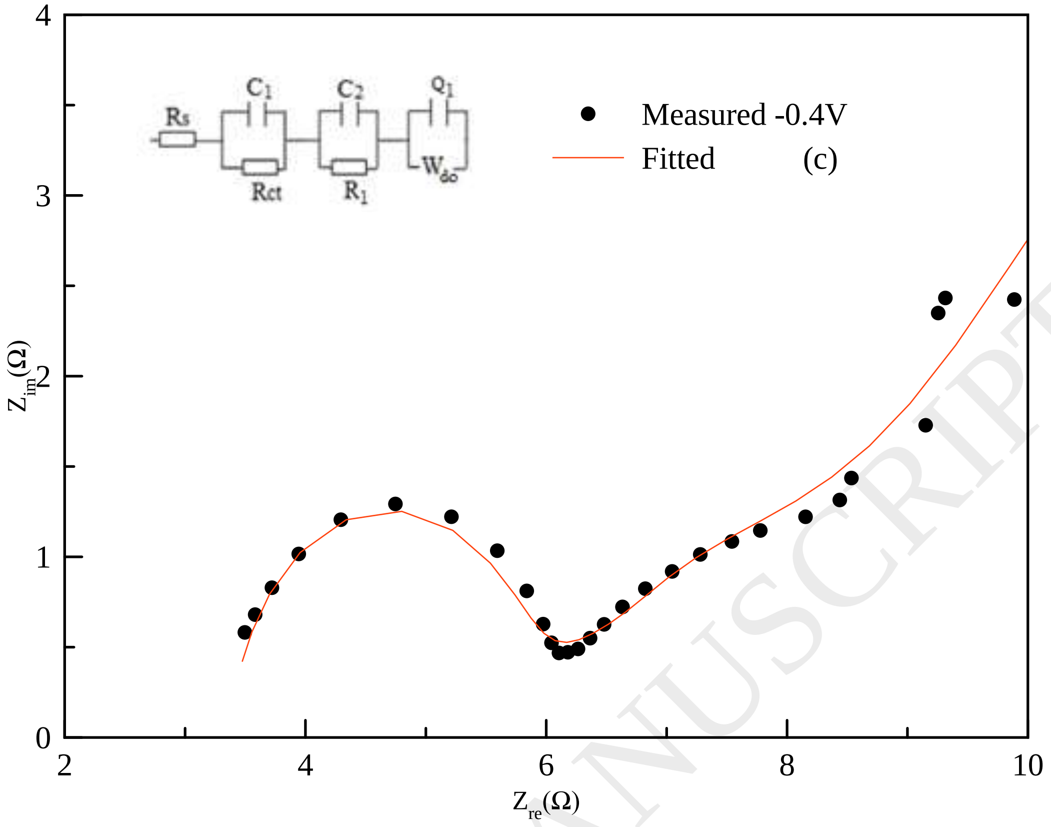
Rs
C1
Rct
C2
R1
Q1
Wdo
Measured -0.4V
Fitted
(c)
4
3
2
1
0
Zim(Ω)
2
4
6
8
10
Zre(Ω)

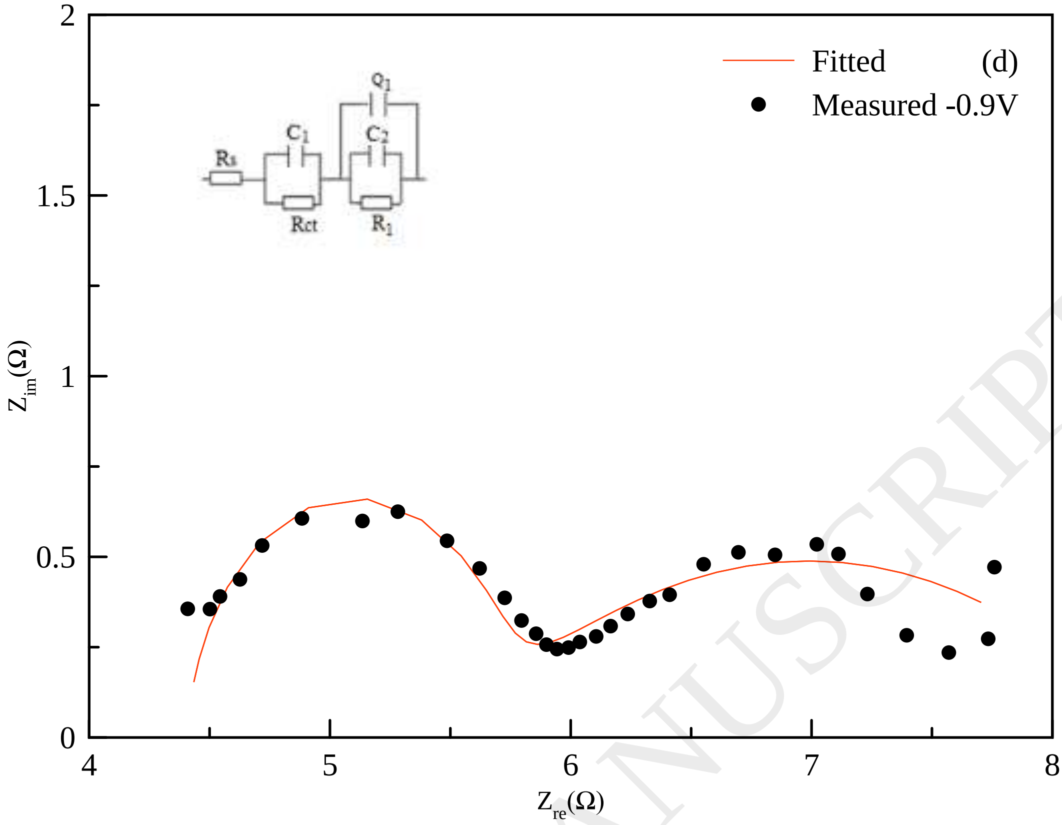

Figure 7 (a) Nyquist plot in the potential range -0.1 to -0.9 V, (b,c,d) Complex plane plot for the impedance corresponding to the simplified Randle's circuit

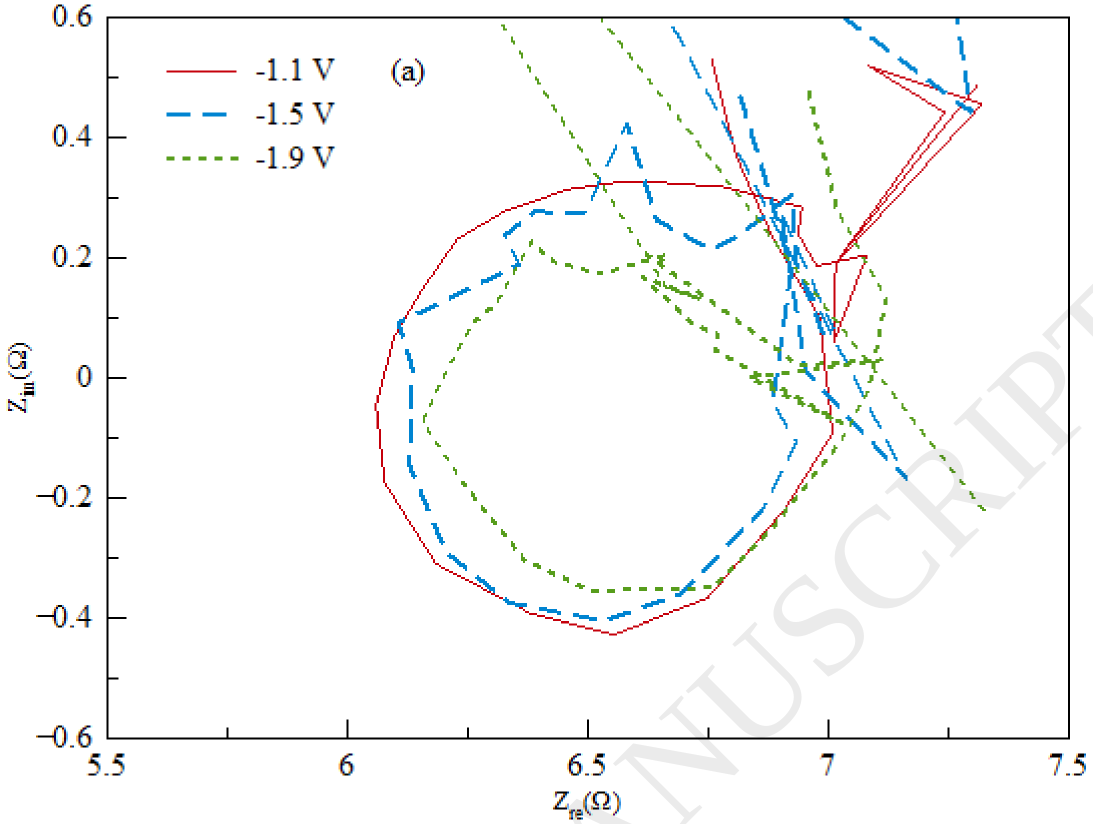
-1.1 V
-1.5 V
-1.9 V
(a)
0.6
0.4
0.2
0
−0.2
−0.4
−0.6
5.5
6
6.5
7
7.5
$Z_{im}(\Omega)$
$Z_{re}(\Omega)$

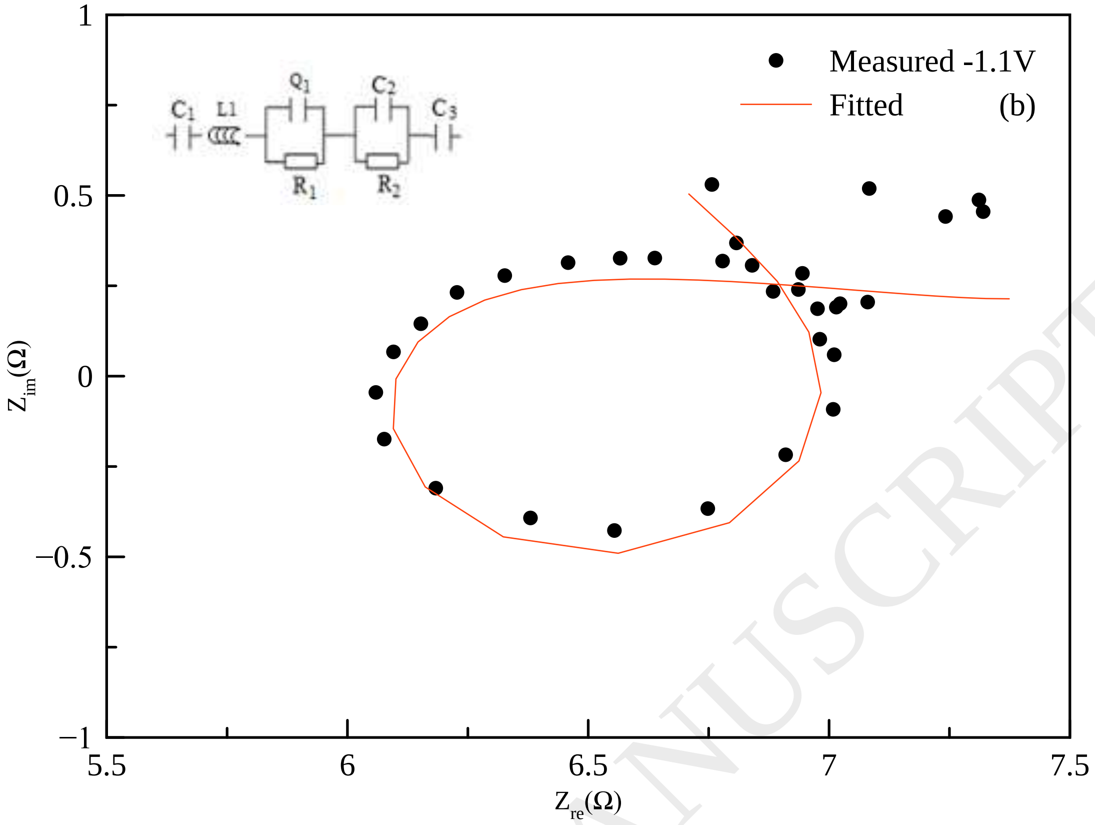

Figure 8 (a) Nyquist plot with inductive behaviour in the potential range -1 to -1.9V, (b) Complex plane plot for the impedance corresponding to the simplified Randle’s circuit

Table 1: Chemical structure and properties four types of amines

Amine	Structure	Proton affinity kJ/mol	Pk$_a$ (ammonium ion)
Ethanolamine (C_2H_7NO)	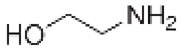	930	9.5±0.15
Diethylenetriamine($C_4H_{13}N_3$)	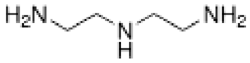	964	10.4±0.05
Diisopropylamine ($C_6H_{15}N$)	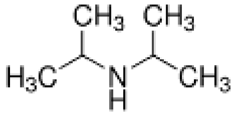	971	11.1±0.01
Aminoethylpiperazine($C_6H_{15}N_3$)	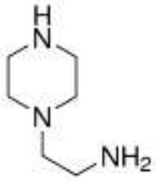	905	8.4±0.012

Table 2. The initial and final pH of DIPA/bicarbonate

concentrationNaHCO$_3$(M)	pHi	pHf
0.1	11.73±0.02	11.69±0.01
0.3	11.16±0.02	11.1±0.02
0.5	10.56±0.01	10.46±0.01
0.7	10.32±0.01	10.2±0.01
1	9.96±0.01	9.78±0.01
0.1	8.0±0.01	8.27±0.01
0.1	9.0±0.02	9.33±0.02
0.1	10.0±0.01	10.47±0.01
0.1	11.0±0.01	11.52±0.01

Table 3 Parameter values of elements in the equivalent circuit model in various potentials

Potential	**R_S** Ω	**R_{CT}** Ω	**R_1** Ω	**C_1** F	**C_2** F	**W_1** $\Omega.\,s^{-0.5}$	**Wd_0/τ_d** Ω	**Q_1** F.s	**n**	**Q_2** F.s	**n**	χ^2
-0.1V	3.42 ±0.01	2.890 ±0.01	9.46 ±0.1	$3.78E^{-6}$ ±2e-4	$3.26E^{-3}$ ±1e-3	38.04 ±0.2		$13E^{-3}$ ±3e-3	0.73			0.017 ±1e-3
-0.4V	3.32 ±0.02	2.21 ±0.01	7.34 ±0.15	$2.25E^{-6}$ ±3e-4	$2.61E^{-2}$ ±1e-3		17.22 / $-7.5E^{-3}$	$71E^{-2}$ ±1e-3	0.25			0.023 ±2e-3
-0.8 V	3.40 ±0.03	2.11 ±0.01	10.04 ±0.13	$2.13E^{-6}$ ±2e-4	$2.25E^{-2}$ ±3e-3			$66E^{-2}$ ±1e-3	0.38			0.014 ±1e-3
-1.1 V	4.22 ±0.02	1.85 ±0.01	1.75 ±0.1			0.206 ±0.01		$28E^{-2}$ ±2e-3	0.65	99E-6 ±1e-4	0.73	0.031 ±3e-3